2950 Niles Road, St. Joseph, MI 49085-9659, USA
269.429.0300 fax 269.429.3852 hq@asabe.org www.asabe.org

An ASABE Meeting Presentation
DOI: https://doi.org/10.13031/aim.202100152
Paper Number: 2100152

Method for aerosolization and collection of Porcine Reproductive and Respiratory Syndrome Virus (PRRSV): engineering considerations

Peiyang Li[1], Jacek A. Koziel[1], Jeffrey J. Zimmerman[2], Steven J. Hoff[1], Jianqiang Zhang[2], Ting-Yu Cheng[2], Wannarat Yim-Im[2], Myeongseong Lee[1], Baitong Chen[1], William S. Jenks[3]*

[1] Department of Agricultural and Biosystems Engineering, Iowa State University, Ames, Iowa, USA
[2] Department of Veterinary Diagnostic and Production Animal Medicine, Iowa State University, Ames, Iowa, USA
[3] Department of Chemistry, Iowa State University, Ames, Iowa, USA

Written for presentation at the
2021 Annual International Meeting
ASABE Virtual and On Demand
July 12–16, 2021

*This paper is modified from a journal paper in Frontiers in Bioengineering and Biotechnology (**doi**: **10.3389/fbioe.2021.659609** publunder CC BY license).*

ABSTRACT. *Porcine reproductive and respiratory syndrome virus (PRRSV) infections cause significant economic losses to swine producers every year. Aerosols containing infectious PRRSV are an important route of transmission, and proper treatment of air could mitigate the airborne spread of the virus within and between barns. Previous bioaerosol studies focused on the microbiology of PRRSV aerosols; thus, the current study addressed the engineering aspects of virus aerosolization and collection. Specific objectives were to (1) build and test a virus aerosolization system, (2) achieve a uniform and repeatable aerosol generation and collection throughout all replicates, (3) identify and minimize sources of variation, (4) verify that the collection system (impingers) performed similarly. The system for virus aerosolization was built and tested (Obj. 1). The uniform airflow distribution was confirmed using a physical tracer (<12% relative standard deviation) for all treatments and sound engineering control of flow rates (Obj. 2). Theoretical uncertainty analyses and mass balance calculations showed a <3% loss of air mass flow rate between the inlet and outlet (Obj. 3). A comparison of TCID50 values among impinger fluids showed no statistical difference between any two of the three trials (p-value = 0.148, 0.357, 0.846) (Obj. 4). These results showed that the readiness of the system for research on virus aerosolization and treatment (e.g., by ultraviolet light), as well as its potential use for research on other types of airborne pathogens and their mitigation on a laboratory scale.*

Keywords. *airborne pathogens, animal production, infectious animal disease, livestock health, mass balance, swine diseases, viral aerosol, virus isolation*

Introduction

Porcine reproductive and respiratory syndrome (PRRS) is one of the most economically impactful diseases that need to be mitigated to ensure animal production security. The annual cost of PRRS to producers was estimated to be $560 million estimated in 2005 (Neumann et al., 2005), $664 million in 2012 (Holtkamp et al., 2013), and $580 million in 2016 (Miller, 2017). The disease is caused by a single-stranded RNA virus (PRRSV), initially described by Terpstra et al. (1991) and Wensvoort et al. (1991).

Air and aerosols are an important route of transmission for some infectious diseases, e.g., foot-and-mouth disease virus (FMDV) (Donaldson et al., 2002) and influenza virus (Herfst et al., 2012). PRRSV can be transmitted via indirect contact (such as aerosol and fomites) or direct contact, but it likewise is found in aerosols generated by infected pigs and reach susceptible pigs meters or kilometers away (Torremorell et al., 1997; Wills et al., 1997; Dee et al., 2005; Otake et al., 2002; Lager and Mengeling 2000; Arruda et al., 2019). Indeed, research suggested that aerosols of infectious PRRSV can travel up to ~9 km (Dee et al., 2009; Otake et al., 2010). The meteorological conditions that favored long-distance transmission of airborne virus included low temperature, moderate levels of relative humidity, rising barometric pressure, low wind speed, and low sunlight intensity (Dee et al., 2010). It was reported that PRRSV could be infectious for 24 h at 37 °C (or 99 °F) and survive for 6 days at 21 °C (or 70 °F) (Pitkin et al., 2017). Given its airborne features and survivability, proper treatment of PRRSV aerosols could effectively reduce the transmission of the disease.

Previous research on the aerosolized PRRSV focused primarily on virus detection and secondarily on engineering, e.g., control of flow rate, pressure, mass balance, and uncertainty analyses. Hermann et al. (2006) optimized a sampling system with six channels for simultaneous PRRSV aerosol recovery and detection. Different sampling devices, parameters, and conditions were compared for optimal airborne virus sampling. Cutler et al. (2012) built upon this work by establishing a PRRSV aerosolization and treatment system with four channels (quartz tubes) for UVC disinfection. Another means of mitigating PRRSV was reported by La et al. (2019), where air ionization was applied on viral aerosols. Systems regarding aerosolization, inactivation, and collection of aerosols were also utilized in studies of other airborne viruses. Welch et al. (2018) established an aerosol exposure chamber (one-channel) where influenza virus was aerosolized, treated by UV, and then sampled by a biosampler; however, that system did not have engineering controls or regulation on airflow rate as well as pressure.

A large gap remains in the knowledge needed to develop effective and practical mitigation technologies for airborne pathogens. In particular, this research requires controlled systems under which mitigation technologies can be tested. We were motivated by the scarcity of research on aerosolized PRRSV and potential limitations of previous data collected without real-time monitoring of an aerosolization system. The objectives of this study were to:

1) build and test a virus aerosolization system,
2) provide a method and protocol of engineering control to regulate pressure and flow rate to ensure uniform aerosol generation and collection throughout all the experiments, as preparation for subsequent research on proper treatment (i.e., UV light) on aerosolized PRRSV,
3) conduct mass balance calculations and uncertainty analyses to minimize variation and validate the system, and
4) conduct PRRSV aerosolization and sampling experiments to verify the equivalency of the impingers.

This research aimed to provide a more quantitative, engineering perspective on controlling the process of aerosolization and collection of viral aerosols to better inform future research on treating aerosols and reduce uncertainty on the collected samples.

Materials and Methods

Experiment Setup (Obj. 1 and 2)

The system (Figure 1, Supplementary Figure 1) mainly consisted of three major sections: (i) aerosolization section, (ii) treatment section, and (iii) sampling section, following the direction of the airflow.

The (i) aerosolization section (Supplementary Figure 2) was responsible for generating PRRSV aerosols that were to be introduced to the treatment section. It included an air compressor (built-in with the fume hood), a pressure regulator, pressure gauges, a mass flow controller (MFC) (model#: GFCS-010013, Aalborg Instruments & Controls Inc., Orangeburg, New York, USA), a 24-jet Collison nebulizer (formerly BGI Inc., now CH Technologies, Westwood, NJ, USA) (Supplementary Figure 3) with the addition of a pressure gauge, and a glass container (12 L, or 3 gals) (Supplementary Figure 4). The pressure regulator included an air filter to remove dust before it came to MFC. The glass container has three channels, two of which were connected with Manifolds (1 and 2), and the 3rd one was closed and considered emergency relief in case the inside pressure was too high for the system to handle (never used in the course of experiments).

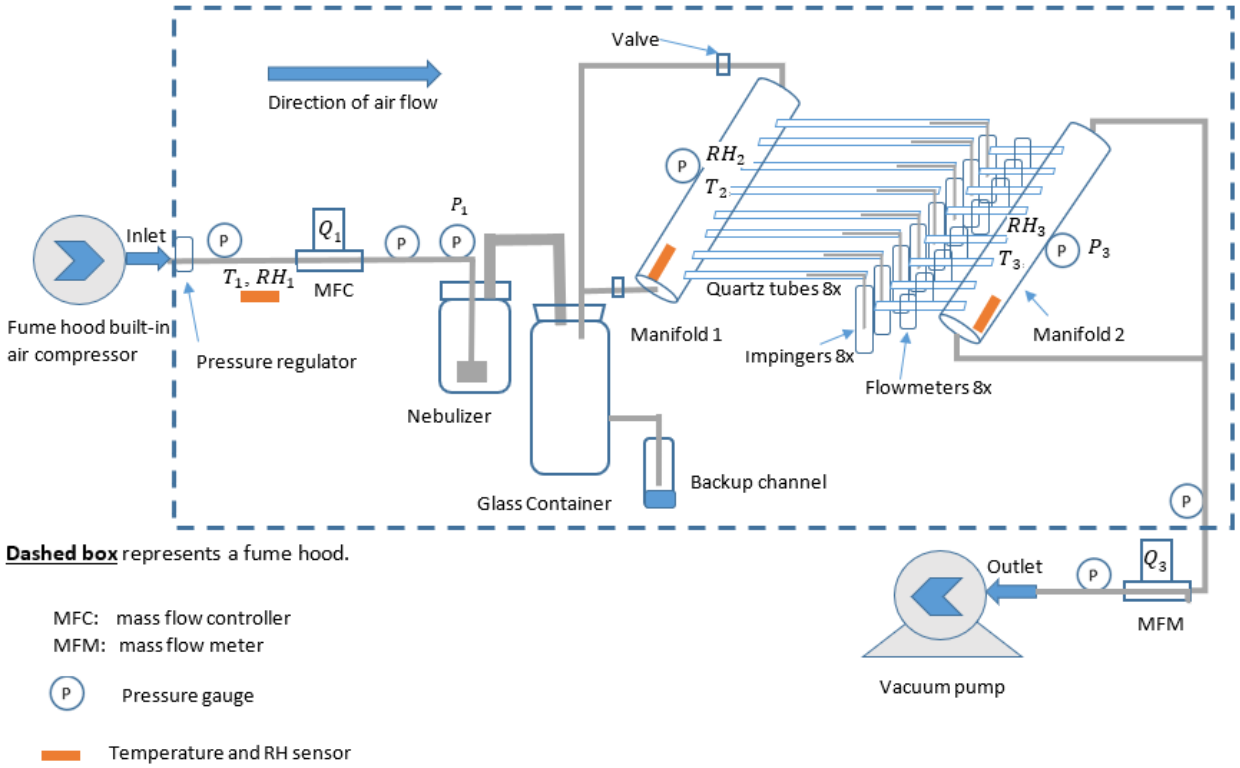

Figure 1. Experimental setup for generation and collection of airborne PRRSV inside a fume hood. The built-in air compressor in the fume hood was responsible for pressurizing air flowing into the system, and the right-side pump was vacuuming exhaust air coming out of the system. MFC = mass flow controller; MFM = mass flow meter. (Published as Figure 1 in Li et al., 2021a under CC BY license).

The (ii) treatment section was designed to be used for subsequent aerosol treatment experiments (such as UV light, filtration, microwave). It included Manifold 1 (with two pressure gauges mounted on top) and all eight branches with quartz tubes and plastic connectors (see the construction of Manifolds 1 and 2 in Supplementary Figures 5 – 8).

The (iii) sampling section was where the aerosols were collected in the sampling media (phosphate-buffered saline, PBS). It consisted of Manifold 2 with eight identical branches connected to eight flowmeters (Catalog No. RMA-21-SSV, Dwyer Instruments Inc., Michigan City, IN, USA) (Supplementary Figures 9 - 10), eight glass AGI 7541 impingers (Ace Glass Inc., Vineland, NJ, USA), pressure gauges, a mass flow meter (MFM) (model#: GFMS-010014, Aalborg Instruments & Controls Inc., Orangeburg, New York, USA), and a vacuum pump (VT 4.16 rotary vane vacuum pump, Becker Pumps Corp., Cuyahoga Falls, OH, USA) (Supplementary Figure 11). The AGI 7541 impingers have a designed flow rate of 6 L/min, and they were tested under experimental conditions where the actual flow rates were verified by Dwyer flowmeters.

All sections of the systems had sensors for temperature (T) and relative humidity (RH) (Table 1). Hose clamps reinforced all the connections between any fitting and plastic tubing to reduce the risk of leakage. According to the MFC and MFM manufacturer, the inlet air needed to be below 70% RH (met this requirement based on measurements) and with a particulate matter (PM) size of < 50 (ensured by the filter in the pressure regulator). Both conditions were met in all trials.

Table 1. Summary of the monitoring sensors in the system and their specifications.

Parameters	Location	Sensor type	Label
Temperature and Relative Humidity	Ambient air	Omega smart temperature and humidity probe	T_1, RH_1
Temperature and Relative Humidity	Manifold 1	Omega smart temperature and humidity probe	T_2, RH_2
Temperature and Relative Humidity	Manifold 2	Omega smart temperature and humidity probe	T_3, RH_3
Pressure	Nebulizer	Analog pressure gauge	P_1
Pressure	Manifold 1	Omega digital pressure gauge	P_2
Pressure	Manifold 2	Omega digital pressure gauge	P_3
Airflow	System Inlet	Aalborg mass flow controller (MFC)	Q_1
Airflow	After impingers	Dwyer flowmeter	Q_{st}

Airflow	System Outlet	Aalborg mass flow meter (MFM)	Q_3

A theoretical model for the mass balance of airflow in virus aerosolization, treatment, and impingement system (Obj. 3)

The theoretical model assumes steady-state conservation of mass and energy during data collection. The purpose of this section is to present the % difference in the mass flow rate of dry air between inlet and outlet in order to detect significant air leakage in the system, to optimize the flow rate, to understand how an aerosolization system would work, and estimate the concentration of PRRSV in the sampling liquid.

Overall mass balance of airflow through the system

A mass balance for dry air is established for the aerosolization and impingement system,

$$\dot{m}_{a1} = \dot{m}_{a3} \quad [1]$$

$\dot{m}_{a1}$ = mass flow rate of dry inlet air (kg_a/s)
$\dot{m}_{a3}$ = mass flow rate of dry outlet air (kg_a/s)

Mass flow rate is the product of the density times volumetric flow rate. Therefore, density and volumetric flow rates need to be determined.

$$\dot{m}_{a1} = \rho_1 Q_1 \quad [2]$$
$$\dot{m}_{a3} = \rho_3 Q_3 \quad [3]$$

ρ_1 = inlet air density (kg_a/m^3)
ρ_3 = outlet air density (kg_a/m^3)
Q_1 = the actual measured flow rate (m^3/s) passing MFC,
Q_3 = the actual measured flow rate (m^3/s) passing MFM,

A general equation to correct the measured flow rate reading on the rotameters according to the pressure enacted on the flowmeter was used (Eqn. 8).

Mass balance of water vapor through the virus nebulizer

The mass balance of moisture through the nebulizer (Figure 2) is:

$$\dot{m}_{a1} w_1 + \dot{m}_{w,nebu} = \dot{m}_{a1} w_2 \quad [4]$$

$\dot{m}_{w,nebu}$ = the change of water vapor content (kg_w/s) caused by the nebulizer
w_1= humidity ratio (kg_w/kg_a) of airflow before nebulizer (Figure 2)
w_2= humidity ratio (kg_w/kg_a) of airflow after nebulizer (Figure 2)

Resulting in the theoretical water vapor content gained during the nebulization process,

$$\dot{m}_{w,nebu} = \dot{m}_{a1}(w_2 - w_1) \quad [5]$$

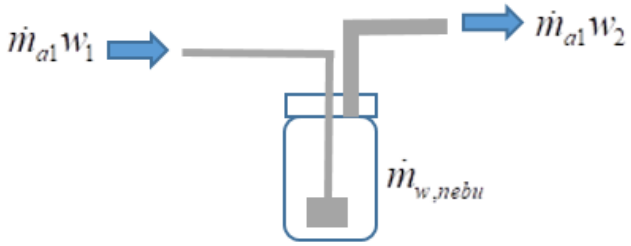

Figure 2. Mass balance of water vapor in the virus nebulizer. The inlet water vapor content plus the water vapor content generated in the nebulizer (from the virus inoculum) is equal to the water vapor content exiting the nebulizer. (Published as Figure 2 in Li et al., 2021a under CC BY license).

An online psychrometric calculator program (Marcks, 2006) was used to calculate the humidity ratio (w) and air density (ρ). The experimental data collected and calculated are within the scope of ANSI/ASHRAE 41.6-1994 (ANSI/ASHRAE, 2006). The input needed to yield these two variables (w, ρ) were the measured relative humidity ($RH_1, RH_2, or\ RH_3$), standard temperature (defined as 21.1 °C, based on instruction manuals from Aalborg and Dwyer), and standard pressure (defined as 14.7 psia, based on instruction manuals from Aalborg and Dwyer).

The air density (ρ) in Eqn. [2] and Eqn. [3] is the air density at standard conditions (21.1 °C and 14.7 psia), 1.19 kg_a/m^3. The variation of RH on ρ under standard conditions is negligible (<1%), and thus the change of ρ was ignored.

Mass balance of water vapor through the impingers

The change of water vapor content across the eight impingers (Figure 3) can be expressed as,

$$\dot{m}_{a1} w_2 + \sum_{n=1}^{8} \dot{m}_{w,impg} = \dot{m}_{a3} w_3 \quad [6]$$

$\dot{m}_{w,impg}$ = the change of water vapor content (kg_w/s) caused by each of the impingers

After rearranging the terms,

$$\sum_{n=1}^{8} \dot{m}_{w,impg} = \dot{m}_{a3}w_3 - \dot{m}_{a1}w_2 \quad [7]$$

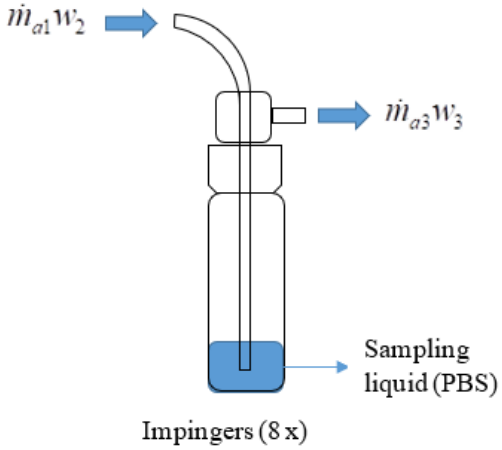

Figure 3. Mass balance of water vapor in the impinger to trap aerosolized virus into sampling liquid. A visual demonstration supplements Eqn. [7]; the water vapor content arriving in the impinger plus the water vapor content absorbed from the sampling liquid is equal to the water vapor content exiting the impinger. (Published as Figure 3 in Li et al., 2021a under CC BY license).

Mass balance of water vapor through the flowmeters (downstream from impingers)

Airflow through each (n=8) of the Dwyer flowmeters, corrected for actual T and P is:

$$Q_{st} = Q_{ob}\sqrt{\frac{P_a \times T_{st}}{P_{st} \times T_a}} \quad [8]$$

Q_{st} = standard flow corrected for pressure and temperature

Q_{ob} = observed flowmeter reading (L/min)

P_a = measured absolute pressure: atmospheric pressure (14.7 psi) ± gauge pressure (psi)

P_{st} = standard pressure (14.7 psi)

T_a = measured temperature (Rankine scale, °R)

T_{st} = standard temperature (530 °R)

Note that in Eqn. [8], all the units under the square root sign are canceled by each other, so the only term that determines the units of this equation is Q_{ob}. This is significant because of Eqn. [8] is also used in the mass balance and uncertainty analyses.

Introducing the constants in equation [8] results in,

$$Q_{st} = Q_{ob}\sqrt{\frac{(14.7+P_a)\times 530}{14.7\times(460+T_a)}} = Q_{ob}\sqrt{\frac{36.0544P_a+530}{T_a+460}} \quad [9]$$

Finally, combining the measurements from all eight flow meters yields,

$Q_{tot} = \sum_{n=1}^{8} Q_{st}$ [10]

In the end, combining Eqns. [1] [5] [7] results in the water vapor balance of each component in the system,

$$\dot{m}_{a1}w_1 + \dot{m}_{w,nebu} + \sum_{n=1}^{8} \dot{m}_{w,impg} = \dot{m}_{a3}w_3 \quad [11]$$

$$\dot{m}_{a1}w_1 + \dot{m}_{a1}(w_2 - w_1) + (\dot{m}_{a3}w_3 - \dot{m}_{a1}w_2) = \dot{m}_{a3}w_3 \quad [12]$$

$\dot{m}_{a1}w_1$= mass flow rate of dry air coming into the system multiplied by the humidity ratio of the air coming into the system

$\dot{m}_{a3}w_3$= mass flow rate of dry air coming out of the impingers multiplied by the humidity ratio of the air coming out of the impingers.

Stabilization of aerosols: calculation of residence time in the glass container

The aerosol residence time refers to the time that an aerosol particle stays in the glass container before it is directed to Manifold 1. Assuming that the glass container is a 'continuous stirred flow reactor' system (Cutler et al., 2013), the mass balance for the concentration of the target substance (e.g., aerosolized virus or tracer) (Table 2) in the container is:

$$V\frac{dC}{dt} = QC_{in} - QC + \emptyset \quad [13]$$

V = volume of the glass container (L),

C = the concentration of the target aerosol in the container,

C_{in} = the concentration of the target aerosol entering the container,

Q = volumetric flow rate (L/min)

$\emptyset$ = addition or subtraction of matters in the container in case of a reaction. In this model, it is assumed that there is no reaction in the container, so $\emptyset = 0$.

t = experiment or operation time (s)

Eqn. [13] can be rearranged to show the change of the aerosol concentration in the container,

$$C = C_{in}(1 - e^{-t\frac{Q}{V}}) \quad [14]$$

The aerosol residence time in the glass container, τ is,

$$\tau = \frac{V}{Q} = \frac{11.4\ L}{48\ L/min} = 0.24\ \text{min} = 14\ s \quad [15]$$

Based on Table 2 and Figure 4, the glass container was assumed to be at a steady-state and contain 99% of the PRRSV aerosols, sufficient for stabilization purposes after 5 τ (70 s) of system operation. Therefore, after 70 s passed, the valves were turned on, and aerosols were directed into Manifold 1.

Table 2. Steady-state conditions. The aerosol concentration with respect to the number of residence times in the glass container.

Time	$\frac{C}{C_{in}}$
1 τ (14 s)	$1 - e^{-1} = 63\%$
2 τ (28 s)	$1 - e^{-2} = 86\%$
3 τ (42 s)	$1 - e^{-3} = 95\%$
4 τ (56 s)	$1 - e^{-4} = 98\%$
5 τ (70 s)	$1 - e^{-5} = 99\%$

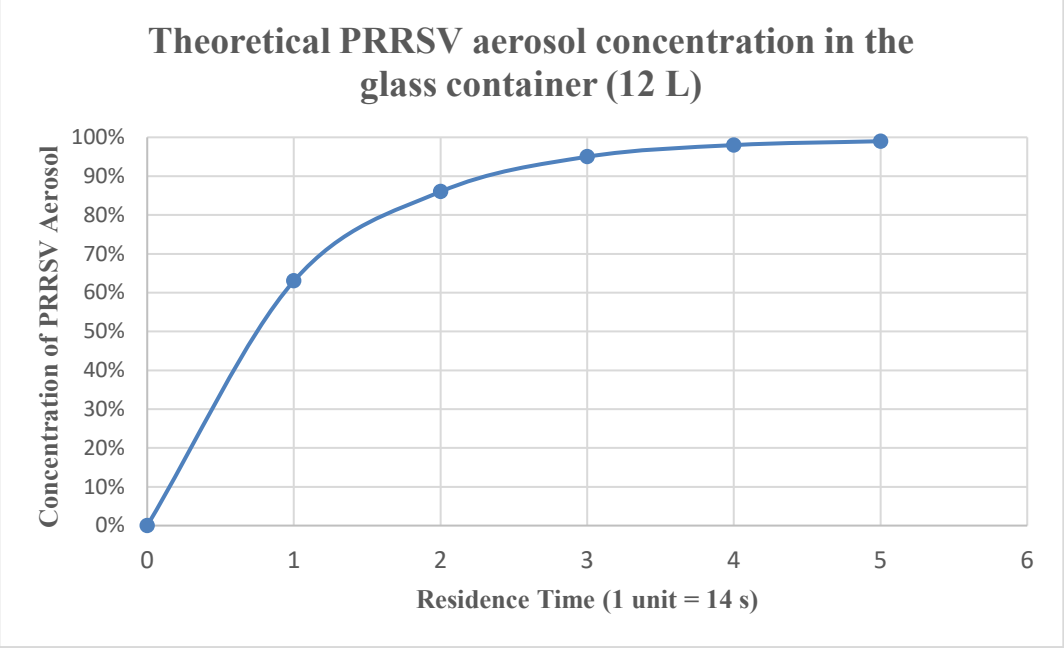

Figure 4. Steady-state conditions for the aerosolized virus. Theoretical PRRSV aerosol concentration in the glass container (12 L) with respect to the operation time (expressed in terms of the aerosol residence time within the glass container). (Published as Figure 4 in Li et al., 2021a under CC BY license).

Uncertainty analysis in the mass balance model (Obj. 3)

First-order error analysis (FOEA), also known as the root sum of squares (RSS) method, was used to present the overall magnitude of measurement uncertainties. In the analysis below, θ refers to the sensitivity of the results, which was calculated by taking the partial derivative regarding each variable, while U refers to the individual measurement uncertainty (composed of both bias errors and precision errors). Adopted from Dettinger and Wilson (1981) and Zhang et al. (2004), the overall uncertainty equation is established as follows,

$$U_{tot} = \sqrt{\sum_1^n (\theta_n U_n)^2} \quad [16]$$

where U_{tot} = total uncertainty of the equipment of study (e.g., a flowmeter).

θ_n= the sensitivity of the nth variable, which is calculated by taking the partial derivative of the equation (e.g., mass balance) with regards to variable n.

U_n= the measurement uncertainty of the *n*th variable in the mass balance equation. This value is usually determined by the manufacturers of the measurement device.

Uncertainty analysis of mass flow in the system inlet and outlet

For the overall system inlet and outlet, the mass flow rates are described in Eqn. [2] and Eqn. [3]. Since ρ_1 and ρ_3 were constants, the uncertainty was determined from Q_1 and Q_3, which were measured by MFM and MFC, respectively. The uncertainty of either one is ±1% of full scale of reading, according to the manufacturers' manual.

For MFC or MFM, the sensitivity and uncertainty of $\dot{m}_{a1}$ with regards to Q_1 are expressed as,

$$\theta_{Q_1} = \frac{\partial \dot{m}_{a1}}{\partial Q_1} = \rho_1 = 1.19\ kg_a/m^3 \quad [17]$$

$$U_{Q_1} = \text{accuracy (\%)} \times F_{MFC} \quad [18]$$

where F_{MFC} = full scale of the MFC (or MFM)

($U_{Q_1} = \pm 1\% \times 48\ L/\min = \pm 0.48\ L/min = 8 \times 10^{-6}\ m^3/s$)

Thus, the total uncertainty of MFC (for inlet), $U_{\dot{m}_{a1}}$ can be summarized as,

$$U_{\dot{m}_{a1}} = \sqrt{\left(\theta_{Q_1} U_{Q_1}\right)^2} \quad [19]$$

The total uncertainty of MFM (for outlet) is the same as MFC because $\rho_1 = \rho_3 = 1.19\ kg_a/m^3$ (based on the assumption made in section 2.2.2), $U_{Q_1} = U_{Q_3} = 4.8 \times 10^{-4}\ m^3/s$, therefore, the calculation is the same as above. In this case, the uncertainty for mass flow inlet and outlet is constant, which does not change due to environmental conditions. Based on the known values and taking them into Eqn. [19], results in $U_{\dot{m}_{a1}} = U_{\dot{m}_{a3}} = 9.52 \times 10^{-6}\ kg_a/s$.

Uncertainty analysis of mass flow through each flowmeter (quartz tube)

The flowrate of each Dwyer flowmeter is expressed as follows (derived from Eqn. [8]),

$$Q_{st} = Q_{ob}\sqrt{\frac{(14.7+P_a)\times 530}{14.7\times(460+T_a)}} = Q_{ob}\sqrt{\frac{36.0544P_a+530}{T_a+460}} \quad [20]$$

The mass flow, $\dot{m}_{a2}$, through each quartz tube is,

$$\dot{m}_{a2} = \rho_2 Q_{ob}\sqrt{\frac{36.0544P_3+530}{T_3+460}} \quad [21]$$

For each of the variables in Eqn. [21], its θ_n (the sensitivity) is calculated by taking the partial derivative of Eqn. [21] with respect to that variable, *n*,

$$\theta_{Q_{ob}} = \frac{\partial \dot{m}_{a2}}{\partial Q_{ob}} = \rho_2\sqrt{\frac{36.0544P_3+530}{T_3+460}} \quad [22]$$

$$U_{Q_{ob}} = \text{accuracy (\%)} \times FS_f \quad [23]$$

where FS_f = full scale of the flowmeter (RMA-21-SSV), and thus $U_{Q_{ob}} = \pm 3\% \times 10\ L/\min = \pm 0.3\ L/min = 5 \times 10^{-6}\ m^3/s$.

$$\theta_{P_3} = \frac{\partial \dot{m}_{a3}}{\partial P_3} = \frac{18.0272 Q_{ob}\rho_2}{\sqrt{(36.0544P_3+530)(T_3+460)}} \quad [24]$$

$$U_{P_3} = \text{accuracy (\%)} \times FS_p \quad [25]$$

where FS_p = full scale of the pressure gauge, and thus $U_{P_3} = \pm 2\% \times 30\ psi = \pm 0.6\ psi$

$$\theta_{T_3} = \frac{\partial Q_{st}}{\partial T_3} = \frac{(-18.0272P_3-265)Q_{ob}\rho_2}{(T_3+460)^2\sqrt{\frac{36.0544P_3+530}{T_3+460}}} \quad [26]$$

$$\theta_{\rho_2} = \frac{\partial Q_{st}}{\partial \rho_2} = Q_{ob}\sqrt{\frac{36.0544P_3+530}{T_3+460}} \quad [27]$$

In addition, $U_{T_3} = \pm 0.2$ ℃ of reading, $U_{\rho_2} = \pm 2.25\%$ of reading.

Thus, the total uncertainty for $\dot{m}_{a2}$, the mass flow through each quartz tube (measured Dwyer flowmeters) is expressed as,

$$U_{\dot{m}_{a2}} = \sqrt{\left(\theta_{Q_{ob,}} U_{Q_{ob}}\right)^2 + \left(\theta_{P_3} U_{P_3}\right)^2 + (\theta_{T_3} U_{T_3})^2 + (\theta_{\rho_2} U_{\rho_2})^2} \quad [28]$$

Example calculation of the uncertainty analysis (Obj. 3)

The summary of measured values for the mass balance model and uncertainty analysis are shown in Table 3.

Table 3. Sample data collection for all variables needed for mass balance and uncertainty analysis.

Location	Variable	Reading	Uncertainty	Measurement Device
Inlet/ambient	T_1, RH_1	21.0 °C, 15.9%	± 0.3 °C of reading, ± 2% of reading	Omega smart temperature and humidity probe
System inlet	Q_1	47.9 L/min	± 1% FS	Aalborg mass flow

				controller
Nebulizer	P_1	21.5 psi	± 0.25% FS	Pressure gauge
Manifold 1	P_2	0 psi	2% FS for the middle half	Pressure gauge
Manifold 1	T_2, RH_2	20.2 °C, 84.6%	± 0.3 °C of reading, ± 2% of reading	Omega smart temperature and humidity probe
Manifold 2	P_3	-4.85 psi	2% FS for the middle half	Vacuum gauge
Manifold 2	T_3, RH_3	20.8 °C, 16.7%	± 0.3 °C of reading, ± 2% of reading	Omega smart temperature and humidity probe
Post-impinger	Q_{ob}	7.25 L/min*	± 3% of reading	Dwyer flowmeter
System outlet	Q_3	49.0 L/min	± 1% FS	Aalborg mass flow meter
Ice buckets**	-	0 ~ 2 °C	N/A	Thermocouples

*The actual flowrate (Q_{st}) was derived from the observed flow rate (Q_{ob}) using Eqn, [8]. In this case, Q_{st} was 5.9 L/min. **Ice bath (container with water and ice mixture) was provided for nebulizer and impingers so that their temperature can be maintained around 0 °C to extend the survivability of PRRSV. Note in Table 3: T_n = temperature (°C); RH_n = relative humidity (%); P_n = pressure (Pa); Q_n = flow rate (L/min); FS = full scale.

Taking the values from Table 3 above into Eqn. [4] and [5] results in $\dot{m}_{a1} = 9.50 \times 10^{-4}\ kg_a/s$, $\dot{m}_{a3} = 9.72 \times 10^{-4}\ kg_a/s$. Therefore, the percentage difference of mass flow between the entire system inlet and outlet was, $\frac{\dot{m}_{a3}-\dot{m}_{a1}}{\dot{m}_{a1}} \times 100\% = 2.32\%$. This indicates relatively low variability and a good mass balance closure. This illustrates sufficient quality control in the assembled and tested virus aerosolization system.

For each quartz connected to a Dwyer flowmeter, based on Eqn. [28], the uncertainty is $U_{\dot{m}_{a2}} = 7.72 \times 10^{-6}\ kg_a/s$. According to Eqn. [21], $\dot{m}_{a2} = 1.18 \times 10^{-4} \pm 7.72 \times 10^{-6}\ kg_a/s$, or $1.18 \times 10^{-4} kg_a/s \pm 6.54\%$. Thus, the uncertainty is minimal, and it does not affect the accuracy of engineering control.

Confirmation of uniform airflow distribution among treatments (Obj. 2 and 4)

Rhodamine B (Sigma-Aldrich Corp., St. Louis, MO, USA), a fluorescent physical tracer (excitation wavelength = 544 nm, emission wavelength = 576 nm) that is not harmful to mammalian cells and viruses (Hermann et al., 2006), was used to confirm the uniformity of the airflow across the eight tubes before the experiments on PRRSV began. Rhodamine B was dissolved in PBS to achieve a concentration of 2 ppm and 60 mL, placed into a 24-jet Collison nebulizer and aerosolized in each experiment. Before each experiment, the system was tested with PBS (no Rhodamine B added), and the Dwyer flowmeters were adjusted to ensure that their readings were the same. After the 10 min experiment, 2 mL of liquid from each impinger was transferred into polystyrene cuvettes (Model# 2405, Stockwell Scientific, Scottsdale, AZ, USA) and warmed up for 10 min in the dark so that they rose to room temperature. The fluorescent intensity was measured by a Modulus Fluorometer (Model 9200-000, Turner Biosystems Inc., Sunnyvale, CA, USA) which was equipped with a green optical kit (Model 9200-042, Turner BioSystems Inc., Sunnyvale, CA, USA). Each sample was distributed into three aliquots (2 mL each), with three measurements each, and the average value was recorded.

PRRSV propagation, isolation, and virus titer determination (Obj. 4)

The PRRSV used in this experiment (MN-184, PRRSV-2 Lineage 1) was provided by the Veterinary Diagnostic Laboratory (College of Veterinary Medicine, Iowa State University). The virus was propagated in the MARC-145 cell line, a clone of the African monkey kidney cell line MA-104 (Kim et al. 1993). MARC-145 cells were cultured in the RPMI-1640 medium supplemented with 10% fetal bovine serum, 2 mM L-glutamine, 0.05 mg/mL gentamicin, 100 unit/mL penicillin, 100 µg/mL streptomycin, and 0.25 µg/mL amphotericin. Large-scale virus propagation was conducted in 5-layer flasks (Thermo Fisher Scientific, Rochester, NY, USA). Briefly, when cells reached 80-90% confluence, stock PRRSV was added. The estimated number of cells at that range of confluency was 18.6-21.0 × 106 cells per layer (Thermo Fisher Scientific, 2021). Flasks were observed daily for cytopathic effect (CPE). When the CPE was abundant (5~7 days), flasks underwent two freeze-thaw cycles, followed by centrifugation at 4,200 × g for 10 min to harvest the supernatant. Approximately 3 L of virus inoculum was harvested with a geometric mean virus titer of $10^{5.56}$ $TCID_{50}$/mL. The inoculum was thoroughly mixed to ensure homogeneity, distributed into 30 mL aliquots, and stored at -80°C.

For determination of $TCID_{50}$ in research samples, impinger fluid was transferred to a biosafety cabinet in a BSL-2 laboratory, and 10-fold serial dilutions were performed, with 8 replicates for each sample. Each well (in 96-well plates) was prefilled with 270 µL of RPMI-1640 medium, and then the sample was added to the first row of the plates; the

solution was mixed, and then 30 µL of liquid transferred sequentially from one row to another. Thus, the dilution for each row ranged from 10^0, 10^{-1}, …, to 10^{-7}, respectively. We considered the 10^0 dilutions to improve method detection limits for the benefit of the subsequent experiments on PPRSV survival after UV treatment. Thereafter, 100 µL from each well was inoculated into 80~90 % subconfluent MARC-145 cells grown in 96-well plates. The plates were incubated at 37 ℃ in a humidified 5% CO_2 incubator. CPE development was checked under a microscope daily, and infected wells were marked as positive until no more additional wells were identified as infected (5 to 7 days). To confirm the presence of PRRSV, the plates were fixed (80% acetone for 10 min), dried, and stained with a PRRSV nucleocapsid protein-specific monoclonal antibody (SDOW17-F) conjugated to fluorescent isothiocyanate (Rural Technologies, Inc., Brookings, SD) for 1 h at 37 °C. The antibody conjugate was decanted, and the cell plates were washed with PBS (1x pH 7.4) 3 times, 5 min each time. Plates were read under an Olympus IX71 fluorescent microscope (Olympus America Inc., Center Valley, PA, USA). The Spearman-Karber method (Karber 1931; Lei et al., 2020) was used to calculate the virus titers, which were based on the number of wells showing positive PRRSV-specific fluorescence at specific dilution and the results expressed as $TCID_{50}$ per mL of the impinger fluid (Cutler et al., 2012; Yim-Im et al., 2021).

Statistical analysis

The statistical analysis was conducted using JMP Pro (Version 15, SAS Institute Inc., Cary, NC, USA). One-way ANOVA and Tukey's test was used to determine statistical significance. p-Values regarding the virus titer were calculated and compared between each combination of two trials (out of the total of three trials). If a p-value was < 0.05, the results were considered significantly different.

Results

Verification of engineering control on airflow rate in the system (Obj. 3)

During each experiment, environmental data such as temperature, pressure, and flow rate were measured and recorded. The results were summarized in Table 4. Table 4 summarized the average values (with +/- standard deviation) of all of the environmental data of the (n = 3) three trials with PRRSV. The purpose of Table 4 is to show the level of engineering control and environmental conditions that the system had, and the variation of the data was indeed minimal. The inlet airflow rate was controlled and measured by the MFC. The inlet air pressure and pressure in the nebulizer were maintained at ~20 psi (1.4 atm).

Table 4. Environmental data for all experimental trials on aerosolization and collection of PRRSV. The system was designed to control and minimize variations of physical parameters.

Environmental Parameters (Mean ± St. Dev.*)			
Engineering-controlled parameters	Inlet air flow rate (L/min), Q_1	47.9 ± 0.4	
	Inlet air pressure (psi), P_1	24.6 ± 0.6	
	The air pressure in the nebulizer (psi), P_2	20.7 ± 0.6	
	The pressure at Manifold 2 (psi), P_3	-4.9 ± 0.4	
	Outlet airflow rate (L/min), Q_3	49.1 ± 0.1	
	Total airflow (L)	2,157.0 ± 16.6	
	Average airflow rate per treatment (L/min)	5.8 ± 0.1	
	Total airflow per treatment (L)	262.5 ± 4.5	
Monitored parameters (uncontrolled)	Ambient air: temperature (℃) & RH (%),T_1, RH_1	21.1 ± 0.7	41.6% ± 6.4%
	Manifold 1 temperature (℃) & RH (%),T_2, RH_2	20.1 ± 0.5	80.0% ± 2.2%
	Manifold 2 temperature (℃) & RH (%), T_3, RH_3	20.6 ± 0.2	36.3% ± 3.8%

* St. Dev.: standard deviation.

Table 5 presents $TCID_{50}$ estimates of PRRSV concentration in the nebulizer and impingers. The comparison showed that a fraction of the PRRSV present in the nebulizer was subsequently recovered in the impingers. This reflects the inactivation of the infectious virus during the process of nebulization, in the aerosolized state, by the process of impingement, and during sample handling, as well as the inefficiency of impingement itself.

Table 5. Measured and estimated $TCID_{50}$ values from the medium in the nebulizer and in impingers.

	Nebulizer	**Impinger (8x)**	**Ratio (Nebulizer/Impinger)**

PRRSV titer * (log_{10}(TCID$_{50}$)/mL)	5.563	3.798 **	58:1
Estimated # of TCID$_{50}$ aerosolized or recovered (log_{10}(TCID$_{50}$))	7.107	5.877	17:1
Description	35 mL of virus inoculum aerosolized for 45 min per experiment	15 mL of medium per impinger (8x in total per experiment)	-

* Estimated as the geometric mean for nebulizer and impingers; ** The geometric mean of PRRSV titer in the impinger fluid from the (n = 3) trials.

Rhodamine B was used as a tracer (positive control) to account for variation among treatments (Table 6). All trials had relative standard deviations (RSD) < 12%. These three trials were independent of the trials mentioned in Table 3, and the only purpose was to evaluate the system integrity before aerosolizing PRRSV. The RSD below 12% for the Rhodamine dye is acceptable in the context of virology research. Inherent variability is assumed for work on biological systems that is generally higher than in engineering fields.

Table 6. Pre-PRRSV experimental verification of air flowrate in each treatment (quartz tubes 1 – 8) with Rhodamine B.

	Prep trial 1		**Prep trial 2**		**Prep trial 3**	
Sample source	**Fluorescent intensity (FSU*)**	**Percentage difference (%) ****	**Fluorescent intensity (FSU*)**	**Percentage difference (%) ****	**Fluorescent intensity (FSU*)**	**Percentage difference (%) ****
Treatment 1	5.11×10^3	-1.3%	5.41×10^3	14.7%	4.09×10^3	0.7%
Treatment 2	4.73×10^3	-8.6%	4.63×10^3	-2.0%	4.91×10^3	20.9%
Treatment 3	4.56×10^3	-12.0%	4.01×10^3	-15.1%	3.56×10^3	-12.5%
Treatment 4	5.70×10^3	10.1%	4.84×10^3	2.6%	3.75×10^3	-7.8%
Treatment 5	5.28×10^3	2.0%	5.02×10^3	6.3%	3.48×10^3	-14.4%
Treatment 6	5.08×10^3	-1.9%	4.50×10^3	-4.7%	4.17×10^3	2.6%
Treatment 7	5.32×10^3	2.8%	4.86×10^3	3.0%	4.53×10^3	11.4%
Treatment 8	5.64×10^3	8.9%	4.49×10^3	-4.9%	4.03×10^3	-0.9%
Mean	5.18×10^3	-	4.06×10^3	-	4.06×10^3	-
St. Dev.***	3.99×10^2	-	4.54×10^2	-	4.54×10^2	-
RSD****	7.7%	-	8.3%	-	11.2%	-

*FSU: Fluorescent standard unit; ** Percentage difference (%): deviated from the average value of the eight samples (of treatments); *** St. Dev.: standard deviation; **** RSD: relative standard deviation.

Verification of the uniformity of airborne PRRSV titer across the treatments (Obj. 3)

The virus titer of the impinger fluid collected from each trial was expressed in the form of $\log_{10}$ normalization (Table 7). Mean, geometric mean, and standard deviations were calculated to evaluate the variability within and between the experimental trials. Data in Table 7 was used to estimate the total geometric mean of PRRSV titer in impingers (i.e., '3.798' reported in Table 5).

Table 7. Experimental verification of uniformity of the PRRSV titer (log_{10}(TCID$_{50}$)/mL) in the sampling fluid among identical eight treatments.

	PRRSV titer (log_{10}(TCID$_{50}$)/mL)		
Sample source	Trial 1	Trial 2	Trial 3
Treatment 1	3.88	3.88	4.00
Treatment 2	3.88	4.13	3.38
Treatment 3	4.13	4.00	3.25
Treatment 4	3.88	3.63	3.63
Treatment 5	3.75	4.13	4.13
Treatment 6	3.88	4.00	3.13
Treatment 7	3.75	3.88	3.63
Treatment 8	3.88	3.63	3.75
Mean ± St. Dev.*	3.88 ± 0.11	3.91 ± 0.18	3.61 ± 0.33

Geo Mean** ± St. Dev.	3.88 ± 0.11	3.90 ± 0.19	3.59 ± 0.33
RSD***	2.8%	4.7%	9.1%
Least Sq Mean	3.88	3.91	3.61
SD Error****	0.085		
Lower 95%	3.70	3.73	3.44
Upper 95%	4.06	4.09	3.79

* St. Dev.: standard deviation; **Geo Mean: geometric mean; ***RSD: relative standard deviation (based on mean and st. dev.); ****SD Error: standard error

Statistical analysis on virus titer (both numerical and $\log_{10}$ based values) was summarized in Table 8.

Table 8. Tukey's test on the statistical significance of the three trials. *P*-values were shown for the three comparisons.

	***p*-value for virus titer ($TCID_{50}$/mL)**	***p*-value for virus titer ($\log_{10}(TCID_{50})$/mL)**
Trial 2 vs. Trial 3	0.1479	0.0560
Trial 1 vs. Trial 3	0.3572	0.0934
Trial 2 vs. Trial 1	0.8458	0.9638

Figure 5 shows the morphological changes of MARC-145 cells under an optical microscope on 3 days post-inoculation of the cells with the sample. In Fig 5A, where cells were inoculated with the control impinge fluid, i.e., virus-negative PBS, no CPE was observed. In contrast, in Fig 5B, where cells were inoculated with the collected PRRSV impinger fluid, CPE characterized by enlargement and clumping of cells was observed. The cell plates were then put back into the incubator for continuous CPE development until 5-7 days post-inoculation. At that time, cells were fixed and stained with FITC-conjugated PRRSV-specific antibodies to confirm the infection status of the cells. Examples of immunofluorescence staining were shown in Figure 6. No immunofluorescence staining was observed in the cells inoculated with the control impinger fluid (Fig 6A). In contrast, in the cells inoculated with the collected PRRSV impinger fluid, positive staining by PRRSV-specific antibody conjugate was clearly observed (Fig 6B).

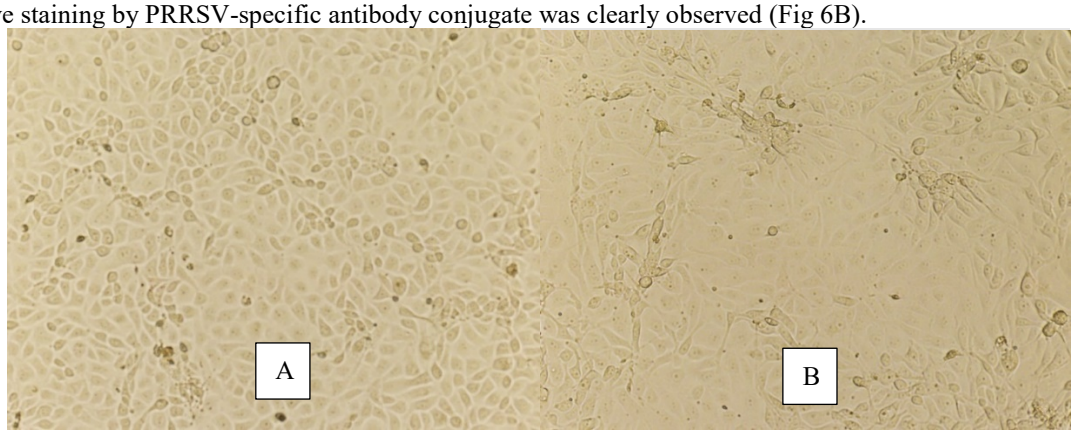

Figure 5. Views of MARC-145 cells at 3 days post-inoculation with control impinger fluid (A) and with the collected PRRSV impinger fluid (B). 160x magnification. (Published as Figure 5 in Li et al., 2021a under CC BY license).

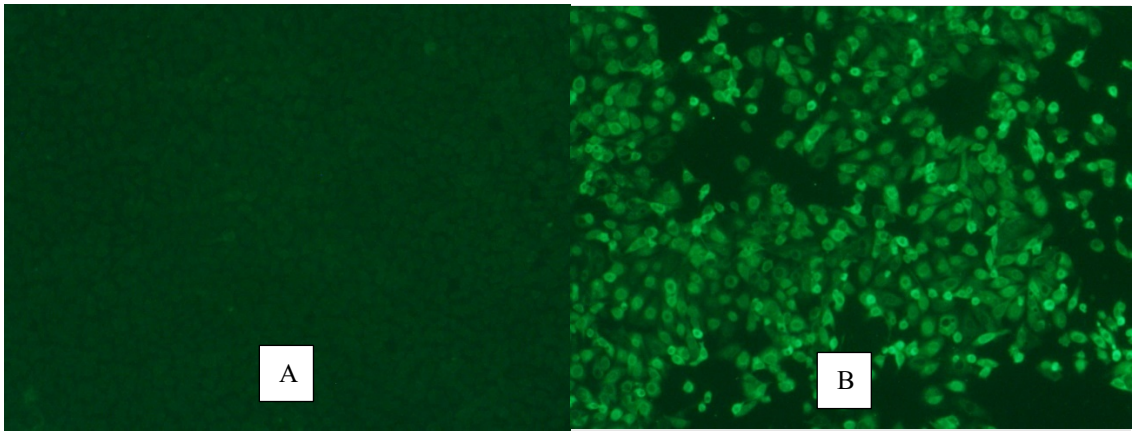

Figure 6. Immunofluorescence staining of cells inoculated with control impinger fluid (A) or PRRSV impinger fluid (B) with PRRSV-specific antibody conjugated to FITC. Pictures were taken on 6 days post-inoculation when the MARC-145 cell plates were fixed using 80% acetone and stained by SDOW-17 PRRSV FITC-conjugate. 160x magnification. (Published as Figure 6 in Li et al., 2021a under CC BY license).

Discussion

Sources of variation

Sources of variation in the data included engineering factors, e.g., sensor measurements (temperature, relative humidity, flow rate), physical tracer (Rhodamine B), and biological factors, e.g., biologically based estimates of virus titer. In the engineering aspect, an uncertainty analysis was conducted with respect to sensor measurements, and the goal was to control and minimize the uncertainty. Ultimately, low variation in the engineering controls minimizes the risks of unacceptable biological variability (which is inherently higher).

Reproducibility

The Rhodamine B fluorometric data supported the conclusion that the airflow was uniform among the eight treatments (tubes) (Table 6), i.e., the RSD among all eight treatments (tubes) was <12%, given all the engineering controls mentioned in the previous sections. However, the absolute values of the fluorescence intensity varied among different trials and cannot be used as verification of flow rate because the variation of flow rate (controlled and verified by MFC, MFM, Dwyer flowmeters) was almost negligible between any two trials (section 2.4).

The PRRSV $TCID_{50}$ estimation of infectious virus is a complex quantal assay that requires (*a*) the propagation of cell cultures, (*b*) inoculation of cells with the virus, and (*c*) visual assessment of the infection of cells by the virus. Despite the biological complexities, $TCID_{50}$ estimates were relatively consistent within and between trials (Table 7).

The system provided acceptable control of flow rate, pressure, and other physical factors while minimizing the potential effect on the micro-infectivity assay. The follow-up research on the inactivation of aerosolized PRRSV using UV-C and UV-A irradiation is described by Li et al., 2021. The same type of studies (aerosolization and recovery) and mitigation could be done using other important airborne pathogens.

Limitations

The system can only control with a flow rate that is < 50 L/min; more specifically, the inlet air flow rate was controlled to be around 48 ± 0.5 L/min. For a higher flow rate, this system would not be practical to handle and would require a redesign, testing, and commissioning similar to the approach presented herein.

The selection of impingers was based on the flow rate, reliability, and cost. Multiple models of impingers were considered, such as SKC BioSampler, AGI 7541, AGI 7542 (also known as AGI 30), etc. Eventually, AGI 7541 was chosen because its designed flow rate is 6 L/min, only half of the designed flow rate of SKC BioSampler or AGI 7542. The lower flow rate impingers allowed for greater flexibility in evaluating UV light's effect on infectious PRRSV in the subsequent research (Li et al., 2021; Koziel et al., 2020). On the one hand, a lower flow rate reduces the efficiency of sampling aerosols. However, on the other hand, a lower flow rate allows more treatment time for the aerosols that are suspended in the air before being captured by the impingers. Thus, the subsequent study (i.e., testing the UV light to inactivate the PRRSV aerosol) benefitted from a wider range of treatment times available (Li et al., 2021; Koziel et al., 2020).

The majority cost of the system was attributed to the sensors, especially the Aalborg MFC and MFM. The Omega Smart Probes were the second most expensive, while the electronic pressure gauges were the third. Some cost savings could be realized by using less expensive sensors (as described in Supplementary Material 1). However, we highly recommend conducting the error propagation and uncertainty analyses as part of the decision-making process.

Overall, the presented system construction and protocol for aerosolization and sampling of PRRSV could be applicable to the aerosolization of other viruses. This experiment could be helpful for future research on virus aerosolization, treatment, and sampling in both human and animal health.

Conclusions

A system for virus aerosolization and protocol for engineering control to regulate pressure and flow rate to ensure uniform aerosol generation and collection was described. The system for virus aerosolization was built and tested (Obj. 1). The uniform airflow distribution was confirmed by the physical tracer (<12% RSD) for all the treatments and sound engineering control of flow rates (Obj. 2). Theoretical uncertainty analysis and mass balance calculation to identify potential variations and reduce them were conducted to prove that a <3% loss of air mass flow rate between the inlet and outlet (Obj. 3). The results showed that the PRRSV titers collected from the impingers were not statistically different, indicating that the variations were acceptable. This indicated the readiness of the system for research on virus aerosolization and treatment (e.g., by ultraviolet light). The $TCID_{50}$ values of the collected impinger fluids showed no statistical difference between any two of the three trials (p-value = 0.148, 0.357, 0.846) (Obj. 4). The presented virus aerosolization system and protocol are also potentially useful for research of other types of airborne pathogens and their mitigation on a laboratory scale.

Conflict of Interest

The authors declare that the research was conducted in the absence of any commercial or financial relationships that could be construed as a potential conflict of interest.

Author Contributions

Conceptualization: JK, JJZ, SH, and WJ; Formal analysis: PL, T-YC, and BC; Funding Acquisition: JK, JJZ, SH, and WJ; Investigation: PL, T-YC, and ML; Methodology: PL, JK, JJZ, JZ, WY-I and T-YC; Resources: JK, JJZ, and JZ; Supervision: JK, JJZ, and JZ; Validation: PL, JK, JJZ, SH, ML, JZ, and WJ; Visualization: PL; Writing – original draft: PL; Writing – review & editing: PL, JK, JJZ, SH, JZ, and WJ.

Funding

This project was funded by checkoff dollars through the National Pork Board (NPB). Project Title: *Mitigation of PRRS transmission with UV light treatment of barn inlet air: proof-of-concept.* Project number: NPB #18-160. In addition, this research was partially supported by the Iowa Agriculture and Home Economics Experiment Station, Ames, Iowa. Project no. IOW05556 (Future Challenges in Animal Production Systems: Seeking Solutions through Focused Facilitation) sponsored by Hatch Act and State of Iowa funds (J.K.).

Acknowledgments

This project was approved by the Institutional Biosafety Committee (IBC) at Iowa State University, and the protocol number is IBC-20-016 (title: *Mitigation of PRRS transmission with UV light treatment of barn inlet air: proof-of-concept)*.

The authors are very thankful to Haiyan Huang (Veterinary Diagnostic Lab staff) for her help on lab skill improvements, Dr. Chumki Banik for her help with purchasing, Danielle Wrzesinski for her help in preparing the experimental setup.

References

Arruda, A. G., Tousignant, S., Sanhueza, J., Vilalta, C., Poljak, Z., Torremorell, M., . . . Corzo, C. A. (2019). Aerosol Detection and Transmission of Porcine Reproductive and Respiratory Syndrome Virus (PRRSV): What Is the Evidence, and What Are the Knowledge Gaps? *Viruses, 11*(8), 712. doi:10.3390/v11080712

ASHRAE Standard 41.6-1994, standard method for measurement of moist air properties. (2006). Atlanta, GA: American Society of Heating, Refrigerating, and Air-Conditioning Engineers.

Cutler, T. D., Wang, C., Hoff, S. J., & Zimmerman, J. J. (2012). Effect of temperature and relative humidity on ultraviolet (UV254) inactivation of airborne porcine respiratory and reproductive syndrome virus. *Veterinary Microbiology, 159*(1-2), 47-52. doi:10.1016/j.vetmic.2012.03.044

Cutler, T. D., Wang, C., Hoff, S. J., & Zimmerman, J. J. (2013). A method to quantify infectious airborne pathogens at concentrations below the threshold of quantification by culture. *Can J Vet Res, 77*(2), 95-99. doi:PMID: 16479728; PMCID: PMC1250242

Dee, S., Batista, L., Deen, J., & Pijoan, C. (n.d.). Evaluation of an air-filtration system for preventing aerosol transmission of Porcine reproductive and respiratory syndrome virus. *Canadian Journal of Veterinary Research = Revue Canadienne De Recherche Veterinaire, 69*(4), 293-298. doi:PMID: 16479728; PMCID: PMC1250242

Dee, S., Otake, S., & Deen, J. (2010). Use of a production region model to assess the efficacy of various air filtration systems for preventing airborne transmission of porcine reproductive and respiratory syndrome virus and Mycoplasma hyopneumoniae: Results from a 2-year study. *Virus Research, 154*(1-2), 177-184. doi:10.1016/j.virusres.2010.07.022

Dee, S., Otake, S., Oliveira, S., & Deen, J. (2009). Evidence of long distance airborne transport of porcine reproductive and respiratory syndrome virus andMycoplasma hyopneumoniae. *Veterinary Research, 40*(4), 39. doi:10.1051/vetres/2009022

Dettinger, M. D., & Wilson, J. L. (1981). First order analysis of uncertainty in numerical models of groundwater flow part: 1. Mathematical development. *Water Resources Research, 17*(1), 149-161. doi:10.1029/wr017i001p00149

Donaldson, A., & Alexandersen, S. (2002). Predicting the spread of foot and mouth disease by airborne virus. *Revue Scientifique Et Technique De L'OIE, 21*(3), 569-575. doi:10.20506/rst.21.3.1362

Herfst, S., Schrauwen, E. J., Linster, M., Chutinimitkul, S., Wit, E. D., Munster, V. J., . . . Fouchier, R. A. (2012). Airborne Transmission of Influenza A/H5N1 Virus Between Ferrets. *Science, 336*(6088), 1534-1541. doi:10.1126/science.1213362

Hermann, J. R., Hoff, S. J., Yoon, K. J., Burkhardt, A. C., Evans, R. B., & Zimmerman, J. J. (2006). Optimization of a Sampling System for Recovery and Detection of Airborne Porcine Reproductive and Respiratory Syndrome Virus and Swine Influenza Virus. *Applied and Environmental Microbiology, 72*(7), 4811-4818. doi:10.1128/aem.00472-06

Holtkamp, D. J., Kliebenstein, J. B., Zimmerman, J. J., Neumann, E., Rotto, H., Yoder, T. K., . . . Haley, C. (2012). Economic Impact of Porcine Reproductive and Respiratory Syndrome Virus on U.S. Pork Producers. doi:10.31274/ans_air-180814-28

Karber, G. (1931). Beitrag zur kollektiven Behandlung pharmakologischer Reihenversuche,. *Arch Exp. Path. Pharmakol, 162*, 480-483.

Kim, H. S., Kwang, J., Yoon, I. J., Joo, H. S., & Frey, M. L. (1993). Enhanced replication of porcine reproductive and respiratory syndrome (PRRS) virus in a homogeneous subpopulation of MA-104 cell line. *Archives of Virology, 133*(3-4), 477-483. doi:10.1007/bf01313785

La, A., Zhang, Q., Levin, D. B., & Coombs, K. M. (2019). The Effectiveness of Air Ionization in Reducing Bioaerosols and Airborne PRRS Virus in a Ventilated Space. *Transactions of the ASABE, 62*(5), 1299-1314. doi:10.13031/trans.13430

Lager, K. M., & Mengeling, W. L. (2000). *Experimental aerosol transmission of pseudorabies virus and porcine reproductive and respiratory syndrome virus* (pp. 409-410). Indianapolis, Indiana: AASP.

Lei, C., Yang, J., Hu, J., & Sun, X. (2020, May). On the Calculation of TCID50 for Quantitation of Virus Infectivity. *Virologica Sinica*.

Li, P., Koziel, J. A., Zimmerman, J. J., Hoff, S. J., Zhang, J., Cheng, T., . . . Jenks, W.S. (2021a). Designing and testing of a system for aerosolization and recovery of viable porcine reproductive and respiratory syndrome virus (PRRSV): theoretical and engineering considerations. *Frontiers in Bioengineering and Biotechnology*, in press. doi: 10.3389/fbioe.2021.659609.

Li, P., Koziel, J. A., Zimmerman, J. J., Zhang, J., Cheng, T., Yim-Im, W., . . . Hoff, S. J. (2021b). Mitigation of Airborne PRRSV Transmission with UV Light Treatment: Proof-of-Concept. Agriculture, 11(3), 259. doi:10.3390/agriculture11030259

Marcks, R. K. (n.d.). Psychrometrics. Retrieved January 17, 2021, from http://daytonashrae.org/psychrometrics/psychrometrics.shtml

Miller, M. (2017, June). Annual PRRS Costs Fall $83.3 Million – Productivity Gains Blunt the Impact of PRRS on the U.S. Herd. *Pork Checkoff Report*, *36*(2), 38-39.

Neumann, E. J., Kliebenstein, J. B., Johnson, C. D., Mabry, J. W., Bush, E. J., Seitzinger, A. H., . . . Zimmerman, J. J. (2005). Assessment of the economic impact of porcine reproductive and respiratory syndrome on swine production in the United States. *Journal of the American Veterinary Medical Association, 227*(3), 385-392. doi:10.2460/javma.2005.227.385

Otake, S., Dee, S. A., Jacobson, L., Pijoan, C., & Torremorell, M. (2002). Evaluation of aerosol transmission of porcine reproductive and respiratory syndrome virus under controlled field conditions. *Veterinary Record, 150*(26), 804-808. doi:10.1136/vr.150.26.804

Otake, S., Dee, S., Corzo, C., Oliveira, S., & Deen, J. (2010). Long-distance airborne transport of infectious PRRSV and Mycoplasma hyopneumoniae from a swine population infected with multiple viral variants. *Veterinary Microbiology, 145*(3-4), 198-208. doi:10.1016/j.vetmic.2010.03.028

Pitkin, A., Dee, S. A., & Otake, S. (2017). Biosecurity protocols for the prevention of spread of porcine reproductive and respiratory syndrome virus. Retrieved January 17, 2021, from http://www.wppa.org/wp-content/uploads/2017/02/PRRSV_BiosecurityManual.pdf

Terpstra, C., Wensvoort, G., & Pol, J. (1991). Experimental reproduction of porcine epidemic abortion and respiratory syndrome (mystery swine disease) by infection with Lelystad vims: Koch's postulates fulfilled. *Veterinary Quarterly, 13*(3), 131-136. doi:10.1080/01652176.1991.9694297

Thermo Fisher Scientific – US. (n.d.). Useful Numbers for Cell Culture. Retrieved March 17, 2021, from https://www.thermofisher.com/us/en/home/references/gibco-cell-culture-basics/cell-culture-protocols/cell-culture-useful-numbers.html

Torremorell, M., Pijoan, C., Janni, K., Walker, R., & Joo, H. S. (1997). Airborne transmission of Actinobacillus pleuropneumoniae and porcine reproductive and respiratory syndrome virus in nursery pigs. *American Journal of Veterinary Research, 58*(8), 828-832. doi:PMID: 9256964

Useful Numbers for Cell Culture. (n.d.). Retrieved March 17, 2021, from https://www.thermofisher.com/us/en/home/references/gibco-cell-culture-basics/cell-culture-protocols/cell-culture-useful-numbers.html

Welch, D., Buonanno, M., Grilj, V., Shuryak, I., Crickmore, C., Bigelow, A. W., . . . Brenner, D. J. (2018). Far-UVC light: A new tool to control the spread of airborne-mediated microbial diseases. *Scientific Reports, 8*(1). doi:10.1038/s41598-018-21058-w

Wensvoort, G., Terpstra, C., Pol, J., Ter Laak, E., Bloemraad, M., De Kluyver, E., . . . Braamskamp, J. (1991). Mystery swine disease in the Netherlands: The isolation of Lelystad virus. *Veterinary Quarterly, 13*(3), 121-130. doi:10.1080/01652176.1991.9694296

Wills, R. W., Zimmerman, J. J., Swenson, S. L., Yoon, K. J., Hill, H. T., Bundy, D. S., & McGinley, M. J. (n.d.). Transmission of PRRSV by direct, close, or indirect contact. Retrieved January 19, 2021, from https://www.aasv.org/jshap/issues/v5n6/v5n6p213.html

Yim-im, W., Huang, H., Park, J., Wang, C., Calzada, G., Gauger, P., . . . Zhang, J. (2020). Comparison of ZMAC and MARC-145 Cell Lines for Improving Porcine Reproductive and Respiratory Syndrome Virus Isolation from Clinical Samples. *Journal of Clinical Microbiology, 59*(3). doi:10.1128/jcm.01757-20

Zhang, H. X., & Yu, S. L. (2004). Applying the First-Order Error Analysis in Determining the Margin of Safety for Total Maximum Daily Load Computations. *Journal of Environmental Engineering, 130*(6), 664-673. doi:10.1061/(asce)0733-9372(2004)130:6(664)